Geophysical Research Letters

RESEARCH LETTER
10.1029/2020GL087860

Evidence of Nighttime Production of Organic Nitrates During SEAC^{4}RS, FRAPPÉ, and KORUS-AQ

Hannah S. Kenagy[1], Tamara L. Sparks[1], Paul J. Wooldridge[1], Andrew J. Weinheimer[2], Thomas B. Ryerson[3], Donald R. Blake[4], Rebecca S. Hornbrook[2], Eric C. Apel[2], and Ronald C. Cohen[1,5]

[1]Department of Chemistry, University of California, Berkeley, CA, USA, [2]Atmospheric Chemistry Observations & Modeling Laboratory, National Center for Atmospheric Research, Boulder, CO, USA, [3]Chemical Sciences Division, NOAA Earth System Research Laboratory, Boulder, CO, USA, [4]Department of Chemistry, University of California, Irvine, CA, USA, [5]Department of Earth and Planetary Science, University of California, Berkeley, CA, USA

Key Points:
- We show evidence for nocturnal production of organic nitrates similar in magnitude to daytime photochemical production
- Significant nocturnal production of organic nitrates observed from three aircraft campaigns in distinct environments
- Nighttime production of organic nitrates impacts our understanding of the nighttime lifetime and fate of NO_x

Supporting Information:
- Supporting Information S1

Correspondence to:
R. C. Cohen,
rccohen@berkeley.edu

Citation:
Kenagy, H. S., Sparks, T. L., Wooldridge, P. J., Weinheimer, A. J., Ryerson, T. B., Blake, D. R., et al. (2020). Evidence of nighttime production of organic nitrates during SEAC^{4}RS, FRAPPÉ, and KORUS-AQ. *Geophysical Research Letters*, *47*, e2020GL087860. https://doi.org/10.1029/2020GL087860

Received 6 MAR 2020
Accepted 16 MAY 2020
Accepted article online 11 MAR 2020

Abstract Organic nitrates ($RONO_2$) are an important NO_x sink. In warm, rural environments dominated by biogenic emissions, nocturnal NO_3-initiated production of $RONO_2$ is competitive with daytime OH-initiated $RONO_2$ production. However, in urban areas, OH-initiated production of $RONO_2$ has been assumed dominant and NO_3-initiated production considered negligible. We show evidence for nighttime $RONO_2$ production similar in magnitude to daytime production during three aircraft campaigns in chemically distinct summertime environments: Studies of Emissions and Atmospheric Composition, Clouds, and Climate Coupling by Regional Surveys (SEAC^{4}RS) in the rural Southeastern United States, Front Range Air Pollution and Photochemistry Experiment (FRAPPÉ) in the Colorado Front Range, and Korea-United States Air Quality Study (KORUS-AQ) around the megacity of Seoul. During each campaign, morning observations show $RONO_2$ enhancements at constant, near-background O_x ($\equiv O_3+NO_2$) concentrations, indicating that the $RONO_2$ are from a non-photochemical source, whereas afternoon observations show a strong correlation between $RONO_2$ and O_x resulting from photochemical production. We show that there are sufficient precursors for nighttime $RONO_2$ formation during all three campaigns. This evidence impacts our understanding of nighttime NO_x chemistry.

Plain Language Summary Nitrogen oxides are pollutants emitted during combustion which are involved in ozone and secondary aerosol production. One way in which nitrogen oxides are removed from the atmosphere is via chemistry that converts them to organic nitrates. This conversion of nitrogen oxides to organic nitrates has been thought to occur primarily during the day when the chemistry is driven by sunlight. Here we show evidence that nighttime processes generate similar quantities of organic nitrates to those produced by sunlight-driven processes.

1. Introduction

Nitrogen oxides ($NO_x \equiv NO + NO_2$) are important tropospheric oxidants that contribute to ozone (O_3) formation, secondary aerosol production, and nitrogen deposition to ecosystems. Alkyl and multifunctional organic nitrates ($RONO_2$) are an oxidative sink of NO_x. Previous studies have shown that $RONO_2$ production is a significant NO_x loss pathway (Day et al., 2003), especially as urban NO_x concentrations decrease (Perring et al., 2013; Romer Present et al., 2020). Organic nitrates can be generated through both daytime photochemical oxidation pathways initiated by OH and nighttime oxidation pathways initiated by NO_3.

During the day, $RONO_2$ is produced photochemically as a radical termination step in a series of reactions between oxidized volatile organic compounds (VOCs) and NO_x (shown in Figure 1). VOCs are oxidized by OH to form organic peroxy radicals, RO_2 (R1). Reaction between NO and organic peroxy radicals can result in formation of an organic nitrate (R2, minor pathway, branching ratio α). The major pathway for the reaction between RO_2 and NO (R3), however, continues radical propagation to form two ozone molecules (R4, R5, R6). Consequently, this daytime chemistry produces both $O_x(\equiv O_3+NO_2)$ and $RONO_2$ so, if photochemistry is dominant, we expect a correlation between O_x and $RONO_2$. Typically, chain lengths are such that we expect 6–20 O_x for each $RONO_2$ (Perring et al., 2013).

©2020. American Geophysical Union. All Rights Reserved.

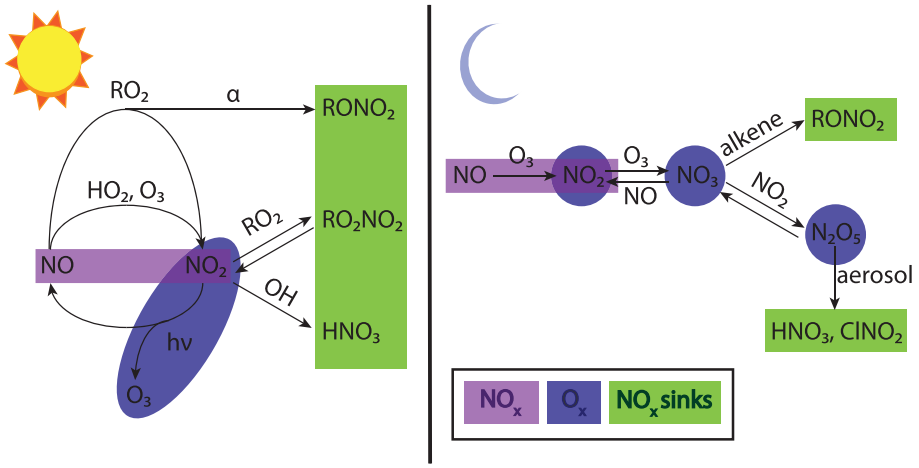

Figure 1. Schematic of daytime (left) and nighttime (right) NO_x chemistry.

$$RH + OH \longrightarrow RO_2 + H_2O \quad (R1)$$

$$RO_2 + NO \longrightarrow RONO_2 \quad (R2)$$

$$RO_2 + NO \longrightarrow RO + NO_2 \quad (R3)$$

$$RO + O_2 \longrightarrow R'(O) + HO_2 \quad (R4)$$

$$HO_2 + NO \longrightarrow OH + NO_2 \quad (R5)$$

$$2NO_2 + h\nu \longrightarrow 2O(^3P) \rightarrow 2O_3 \quad (R6)$$

At night, $RONO_2$ is produced from alkenes via addition of NO_3 to a double bond (R9), as shown in Figure 1. NO_3 is formed from reaction between NO_2 and O_3 (R8). During the day, NO_3 is lost quickly via reaction with NO or via photolysis. In the nocturnal residual layer removed from fresh NO emissions, NO_3 concentrations can build up and react with alkenes. Two O_3 molecules are consumed in the production of NO_3 (R7 followed by R8), meaning that nighttime $RONO_2$ formation is a net sink of O_x. Consequently, we do not expect a positive correlation between $RONO_2$ and O_x if NO_3 is the dominant oxidant, and we might even expect a weak negative correlation.

$$NO + O_3 \longrightarrow NO_2 \quad (R7)$$

$$NO2 + O_3 \longrightarrow NO_3 + O_2 \quad (R8)$$

$$NO_3 + R_1 = R_2 \longrightarrow R_1(ONO_2) - R_2 \quad (R9)$$

The fate of NO_x at night is controlled by the balance of two NO_3 reaction pathways. First, NO_x can be lost via NO_3 reaction with alkenes, as described above. Second, NO_3 can be lost at night via reaction with NO_2 to form N_2O_5 in thermal equilibrium, followed by aerosol uptake and heterogeneous hydrolysis to produce HNO_3 and $ClNO_2$. In certain environments, NO_3 may also react with species such as dimethyl sulfide, aldehydes, and peroxy radicals. The competition between these reaction pathways is controlled by both the relative availability of alkenes and by the fate of N_2O_5. Nighttime $RONO_2$ production increases in environments with high biogenic alkene emissions (isoprene, monoterpenes) and in environments with high anthropogenic alkene emissions, particularly where either of these two emission sources is sustained overnight. The N_2O_5 loss pathway becomes less competitive with $RONO_2$ formation in environments with

low aerosol surface area and small heterogeneous uptake coefficients for N_2O_5 ($\gamma(N_2O_5)$), as these decrease the rate of heterogeneous hydrolysis of N_2O_5. Additionally, higher temperatures shift the N_2O_5 equilibrium towards dissociation, making N_2O_5 formation less favorable, while also increasing the rate of bimolecular NO_3 reactions with alkenes. Thus, nighttime $RONO_2$ formation is most favorable in environments with high alkene emissions, low aerosol surface area, small $\gamma(N_2O_5)$, and high temperature.

There is reason to suspect that $RONO_2$ production from nighttime NO_3 oxidation of VOCs could be competitive with $RONO_2$ production from photochemical OH oxidation. Because it is removed from fresh overnight NO emissions, a chemically active residual layer characteristic of many nighttime environments can contain elevated NO_3 concentrations as well as VOC emissions from late in the day. Moreover, $RONO_2$ yields from NO_3-initiated oxidation (20–80%) are far larger than $RONO_2$ yields from OH-initiated oxidation of VOCs (0.1–35%) (Perring et al., 2013 and references within). Even if NO_3 oxidation represents a smaller fraction of total VOC oxidation than OH oxidation, the larger $RONO_2$ yields could make $RONO_2$ production from NO_3 oxidation competitive with $RONO_2$ production from OH oxidation.

A number of recent studies have shown that NO_3 oxidation can be a significant source of $RONO_2$ in regions dominated by biogenic VOC emissions. In forested regions of Colorado, Finland, and Germany, nighttime concentrations of $RONO_2$ were found to be comparable with daytime $RONO_2$ concentrations (Fry et al., 2013; Liebmann et al., 2019; Sobanski et al., 2017). Other studies have found NO_3-initiated formation of isoprene nitrates to be competitive with OH-initiated formation of isoprene nitrates in the Southeastern United States (Starn et al., 1998; Xiong et al., 2015), in an observationally constrained model of the eastern United States (Horowitz et al., 2007), and in a global model (von Kuhlmann et al., 2004).

Moreover, NO_3 oxidation has been shown to be a significant source of organic aerosol in the Central Valley of California (Rollins et al., 2012), the Southeastern United States (Ayres et al., 2015; Fisher et al., 2016; Lee et al., 2016; Pye et al., 2015; Xu, Guo et al. 2015; Xu, Suresh et al. 2015), in a forested region of Colorado (Fry et al., 2013), in rural Southwestern Germany (Huang et al., 2019), throughout Europe (Kiendler-Scharr et al., 2016), and in the Alberta oil sands (Lee et al., 2019).

Though NO_3 chemistry has been shown to be an important source of $RONO_2$ and secondary organic aerosol in rural regions dominated by biogenic emissions, nocturnal NO_3-initiated $RONO_2$ formation has often been considered negligible in comparison with daytime OH-initiated production of $RONO_2$ in urban environments. In this study, we present evidence for significant nighttime $RONO_2$ production using measurements of O_x and $RONO_2$ from three aircraft-based field campaigns in distinct summertime environments. First, we show evidence for significant nighttime $RONO_2$ production in the rural southeastern United States during Studies of Emissions and Atmospheric Composition, Clouds, and Climate Coupling by Regional Surveys (SEAC^{4}RS), an area with high biogenic emissions. Second, we show similarly high nighttime $RONO_2$ production in two urban areas: in the Colorado Front Range during Front Range Air Pollution and Photochemistry Éxperiment (FRAPPÉ), which is affected by both high urban and oil/gas emissions, as well as in and around the megacity of Seoul during Korea-United States Air Quality Study (KORUS-AQ). In each location, we show that the expected linear relationship between O_x and $RONO_2$ is observed during the afternoon. However, during the morning hours, the relationship between O_x and $RONO_2$ shows evidence of nighttime $RONO_2$ production. We support this conclusion further by assessing precursor availability for nighttime $RONO_2$ production.

2. Measurements

2.1. SEAC^{4}RS, FRAPPÉ, and KORUS-AQ Aircraft Campaigns

The SEAC^{4}RS campaign took place during August and September 2013 in the Southeastern and Western United States (Toon et al., 2016). This analysis uses observations from the NASA DC-8 aircraft which flew 19 primarily daytime research flights out of Ellington Field, near Houston, TX.

The FRAPPÉ campaign took place during July and August 2014 in the Northern Front Range Metropolitan Area (NFRMA) of Colorado (Flocke et al., 2020). This analysis uses observations from the NSF/NCAR C-130 aircraft which flew 15 daytime research flights out of the Rocky Mountain Metropolitan Airport in Jefferson County, CO.

The KORUS-AQ campaign took place during May and June 2016 over South Korea and the Yellow Sea (Nault et al., 2018). This analysis uses observations from the NASA DC-8 aircraft which flew 20 daytime research flights out of Pyeongtaek, South Korea (≈60 km south of Seoul).

2.2. Instrumentation

During all three campaigns, measurements of NO_2 and total $RONO_2$ (including both gas-phase and particle-phase $RONO_2$) were made by the UC Berkeley thermal dissociation laser-induced fluorescence (TD-LIF) instrument (Day et al., 2002; Wooldridge et al., 2010). Briefly, one channel of the instrument measures NO_2 by laser-induced fluorescence. Two other channels first flow air through a heated quartz oven. One channel is set at 180°C, the temperature at which peroxy nitrates (RO_2NO_2) dissociate into RO_2 and NO_2. The second is set at 360°C, the temperature at which $RONO_2$ dissociate into RO + NO_2. The difference in NO_2 detected in adjacent channels gives the mixing ratio for each class of compounds: the RO_2NO_2 mixing ratio is the difference between the 180°C channel and the unheated channel, and the $RONO_2$ mixing ratio is the difference between the 360°C channel and the 180°C channel.

O_3 and NO were measured by chemiluminescence. During SEAC^{4}RS, O_3 and NO were measured by the NOAA NO_yO_3 instrument (Ryerson et al., 1999, 2000). During FRAPPÉ and KORUS-AQ, O_3 and NO were measured by the NCAR chemiluminescence instrument (Ridley et al., 1994; Weinheimer et al., 1994).

Alkenes were measured by whole air sampling (WAS) (Colman et al., 2001; Simpson et al., 2011) and trace organic gas analyzer (TOGA) (Apel et al., 2015). For SEAC^{4}RS and KORUS-AQ, we use WAS measurements of propene, butenes, isoprene, α-pinene, and β-pinene. During FRAPPÉ, we use WAS measurements of propene, isoprene, α-pinene, and β-pinene and TOGA measurements of butenes and limonene.

Instrument details, including accuracy and sampling interval, can be found in Table S1 of the Supporting Information. We use 1-min averaged data, and we consider only boundary layer data (below 1 km during SEAC^{4}RS and KORUS-AQ and below 2 km during FRAPPÉ).

3. Observations/Results

3.1. O_x versus $RONO_2$

The relationship between O_x and $RONO_2$ during each campaign is shown in Figure 2 (plots of the relationship between O_x and $RONO_2$ during each flight within each each campaign are shown in Figures S1–S6). During all three campaigns, during the afternoon hours (13:00–19:00 local time) when photochemistry is most active, there is a positive, linear relationship between O_x and $RONO_2$, indicating that photochemical production of both O_x and $RONO_2$ is occurring. The slope of the relationship between O_x and $RONO_2$ mixing ratios is indicative of the branching ratio between O_x and $RONO_2$ production. From Figure 2, during SEAC^{4}RS, 29 O_x are produced for each $RONO_2$. Chain lengths are shorter during FRAPPÉ, where 13 O_x are produced for each $RONO_2$, and longer during KORUS-AQ, where 43 O_x are produced for each $RONO_2$.

During the morning hours (before 11:00 local time) before peak photochemistry occurs, however, the relationship between O_x mixing ratios and $RONO_2$ mixing ratios has a flat (zero) slope. At a relatively constant observed O_x mixing ratio, a wide range of $RONO_2$ mixing ratios was observed. This indicates that O_x and $RONO_2$ are not produced from the same pathway. Instead, the high levels of $RONO_2$ at relatively low levels of O_x suggest that much of the observed $RONO_2$ was produced via a non-photochemical pathway that produces $RONO_2$ without generating O_x. Since this trend is only observed in the morning, and not in the afternoon, it is indicative of a large source of $RONO_2$ produced from NO_3 oxidation overnight.

We also explored the effects of O_3 deposition and nighttime dynamics, but neither could sufficiently explain the observed trend. Estimating an approximate O_3 deposition velocity of 0.5 cm s^{-1} (e.g.,Colbeck & Harrison, 1985; Lenschow et al., 1981) and boundary layer height of 1 km, the lifetime of O_3 to deposition is 56 h, far longer than the chemical timescales relevant to this analysis. Entrainment of air from aloft could also affect observed morning mixing ratios, but would have the same relative effect on both O_3 and $RONO_2$. Consequently, neither O_3 deposition nor entrainment can explain the lack of correlation between O_x and $RONO_2$ in the morning; the observed effect can only be explained by significant nocturnal production of $RONO_2$.

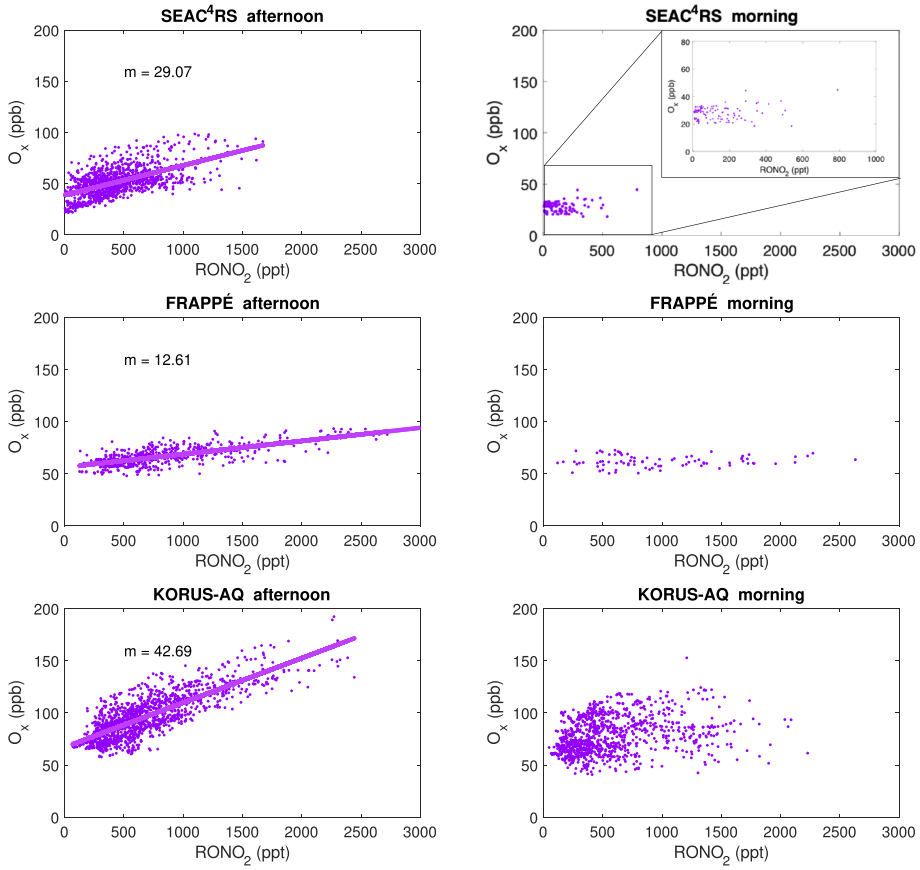

Figure 2. Plots of O_x vs. $RONO_2$ during SEAC[4]RS, FRAPPÉ, and KORUS-AQ during afternoon (left, 13:00–19:00 local time) and morning (right, before 11:00 local time). Only data in the boundary layer (<1 km for SEAC[4]RS and KORUS-AQ, <2 km for FRAPPÉ) are included. York linear fits (with slopes labeled as *m*) to the afternoon data are shown.

3.2. Precursors for Nighttime $RONO_2$ Production

As additional evidence for nighttime $RONO_2$ production, we assess the availability of precursors to $RONO_2$ production, namely NO_3 and alkenes. We report average morning (before 11:00 local time) mixing ratios of $RONO_2$, alkenes, and NO_x in Table 1. The abundance of NO_x and alkenes observed in the morning indicates that these precursors are not depleted by overnight chemistry; rather, the non-zero concentrations of precursors in the morning suggests that NO_3-initiated $RONO_2$ production chemistry is sustained overnight and occurs until daybreak.

During SEAC[4]RS, there were insufficient morning alkene measurements to report meaningful averages. However, Edwards et al. (2017) report airborne measurements which show that the nocturnal residual layer in the Southeastern United States is rich in isoprene, evidence that there is an abundance of alkenes available overnight to form alkyl nitrates.

Moreover, we use the observed morning mixing ratios of NO_x, O_3, and alkenes to calculate lower bounds on the integrated overnight production of NO_3 (Equation 1), the instantaneous production rate of $RONO_2$ (Equation 2), and the instantaneous production rate of alkenes + O_3 (Equation 3).

$$\int P(\mathrm{NO_3}) = \mathrm{NO_{x,\mathit{initial}}}(1 - \exp(-t \times k_{\mathrm{NO_2+O_3}} \times [\mathrm{O_3}])) \quad (1)$$

$$P(\mathrm{RONO_2}) = \Sigma_i \alpha_i \times k_{\mathrm{NO_3+alkene}_i} \times [\mathrm{alkene}_i] \times [\mathrm{NO_3}] \quad (2)$$

$$\mathit{Rate}(\mathrm{O_3 + alkene}) = \Sigma_i k_{\mathrm{O_3+alkene}_i} \times [\mathrm{alkene}_i] \times [\mathrm{O_3}] \quad (3)$$

Table 1
Table of the Average $RONO_2$, Alkene, and NO_x Concentrations in the Morning (Before 11:00 Local Time), Integrated Overnight Production of NO_3, Instantaneous Production Rate of $RONO_2$, and Instantaneous Reaction Rate of Alkenes with O_3

	SEAC^{4}RS	FRAPPÉ	KORUS-AQ
$RONO_2$ (ppb)	0.12	0.98	0.56
propene (ppt)	N/A	98	129
butene (ppt)	N/A	39	60
isoprene (ppt)	N/A	109	54
α-pinene (ppt)	N/A	11	15
β-pinene (ppt)	N/A	9.0	11
limonene (ppt)	N/A	4.8	N/A
NO_x (ppb)	0.43	8.1	4.4
$\int P(NO_3)$ (ppb)[a]	0.23	5.2	2.9
$P(RONO_2)$ (ppb/h)[a,b,c]	N/A	2.3	1.3
alkene + O_3 rate (ppb/h)[a,b]	N/A	0.021	0.108

Note. There are insufficient morning SEAC^{4}RS measurements due to data sparsity to report meaningful morning average alkene mixing ratios. [a]Calculated from morning (before 11:00 local time) precursor observations and can therefore be considered a lower bound. [b]Rate constants from MCM v3.3.1 are used. [c]Nitrate yields used are from Perring et al. (2013) and references therein.

As shown in Table 1, the integrated production of NO_3 exceeds the observed morning mixing ratios of $RONO_2$, and the production rates of $RONO_2$ calculated from morning observations are more than sufficiently fast to account for the morning observations of $RONO_2$. Lastly, the rate of VOC (ethyne, ethene, propene, MACR, MVK, isoprene, butene, α-pinene, β-pinene, and limonene) oxidation by O_3 is at least an order of magnitude smaller than the production rate of $RONO_2$, indicating that NO_3 is the dominant nocturnal alkene oxidant in these environments.

4. Discussion and Conclusion

We show evidence of significant nighttime $RONO_2$ production during three aircraft campaigns in three distinct locations: the rural southeastern United States dominated by biogenic emissions (SEAC^{4}RS), the Colorado Front Range dominated by a combination of urban and oil/gas emissions (FRAPPÉ), and the megacity of Seoul dominated by urban emissions (KORUS-AQ). Though, in urban areas, nighttime production of $RONO_2$ has often been considered negligible in comparison with daytime production, we show evidence for nighttime $RONO_2$ production that results in morning $RONO_2$ mixing ratios of similar magnitude to afternoon observations of $RONO_2$ in all three of these distinct environments.

Rapid nighttime $RONO_2$ production impacts our understanding of the lifetime and fate of NO_x at night. Evidence for nighttime $RONO_2$ production indicates that HNO_3 and $ClNO_2$ produced via heterogeneous hydrolysis of N_2O_5 are not necessarily the dominant nighttime sinks of NO_x, consistent with other aircraft-based nighttime urban NO_3 budgets (Brown et al., 2011). In environments with low aerosol loading, high temperatures, and an abundance of alkenes, $RONO_2$ production can be the dominant nighttime NO_x sink. Significant nocturnal NO_3-initiated $RONO_2$ production in urban areas also has implications for substantial overnight secondary organic aerosol production in and around cities.

We explore the effects of temperature, alkenes, and aerosol surface area on the fraction of NO_x lost as $RONO_2$ (defined as $\frac{P(RONO_2)}{P(RONO_2)+P(HNO_3)}$) at night in Figure 3, assuming an initial NO_2 concentration, constant O_3, pressure, and $\gamma(N_2O_5)$, and NO_3 and N_2O_5 in steady state (see Appendix A). Under these model conditions, the temperature, pressure, alkenes, NO_2, O_3, and aerosol surface area measured in the evening (after 16:30 local time) during FRAPPÉ and SEAC^{4}RS indicate that $RONO_2$ is the dominant sink of NO_x at night and during KORUS-AQ indicate that overnight NO_x loss is evenly split between N_2O_5 loss and $RONO_2$ production. This is consistent with a tower-based measurement in Seoul in 2015 which showed rapid NO_3-BVOC chemistry (Brown et al., 2017). For contrast, during the WINTER campaign (aircraft campaign over NE US, February to March 2015), low temperatures and low alkene concentrations lead to NO_x loss at night dominated by

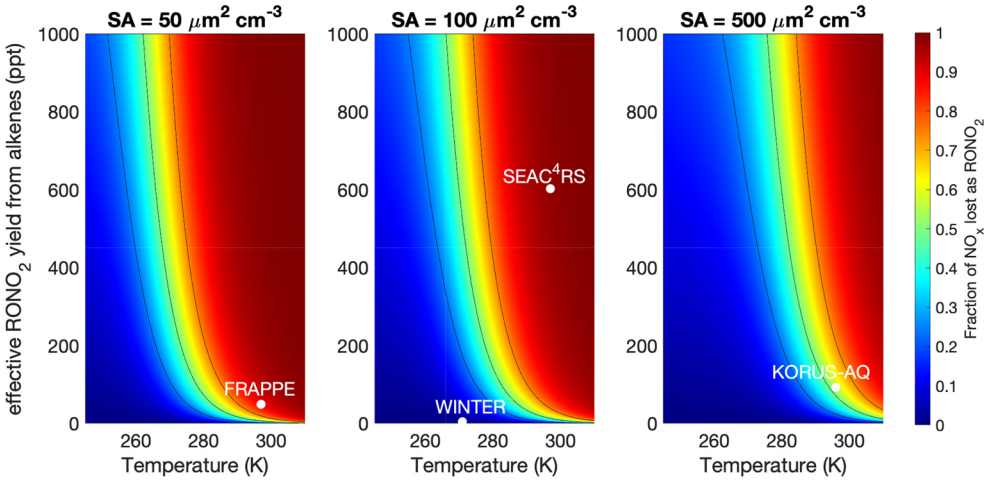

Figure 3. Fraction of NO_x lost as $RONO_2$ (defined as $\frac{P(RONO_2)}{P(RONO_2)+P(HNO_3)}$ overnight), shown as a function of temperature and effective $RONO_2$ yield from alkenes ($\Sigma_i \alpha_i[\text{alkene}]_i$) for three different aerosol surface areas (SA = 50, 100, and 500 $\mu m^2 cm^{-3}$). We assume an initial NO_2 concentration (1 ppb), constant O_3 (40 ppb), constant pressure (1013 hPa), constant $\gamma(N_2O_5)$ (0.04), and NO_3 and N_2O_5 in steady state. Black contour lines correspond to 25%, 50%, and 75% of NO_x lost as $RONO_2$. Average evening (after 16:30 local time) conditions during SEAC^{4}RS, FRAPPÉ, and KORUS-AQ are shown. Average conditions during WINTER (NSF aircraft campaign over Northeastern United States during February to Mar 2015) are also shown as an example of conditions during which N_2O_5 loss is the dominant nighttime sink of NO_x (Kenagy et al., 2018).

N_2O_5 hydrolysis (Kenagy et al., 2018). Histograms of the distribution of the fraction of NO_x lost as $RONO_2$ calculated from evening observations of NO_2, O_3, alkenes, temperature, and pressure during each campaign can be found in Figures S7–S9.

Here we have presented evidence for a significant, and sometimes dominant, nighttime source of $RONO_2$ using airborne, daytime measurements. Further measurements of the diel cycles of $RONO_2$ and its precursors would be of use to further elucidate the relative importance of the different mechanisms for $RONO_2$ formation. Additionally, measurements of the diel cycle of $RONO_2$ could provide insights into the fate of daytime- and nighttime-produced $RONO_2$ by showing whether they remain in the gas phase or partition into particles and whether hydrolysis, oxidation, or deposition dominates loss of $RONO_2$.

Appendix A: Calculating Fraction of NO_x Lost as $RONO_2$ Overnight

We calculate the nighttime production of $RONO_2$ from reaction of NO_3 and alkenes (R9) and the nighttime loss of N_2O_5 from heterogeneous hydrolysis (approximated as production of HNO_3) as

$$P(\text{RONO}_2) = \Sigma_i \alpha_i \times k_{\text{NO}_3 + \text{alkene}_i} \times [\text{alkene}_i] \times [\text{NO}_3] \quad \text{(A1)}$$

$$P(\text{HNO}_3) = k_{hyd}[\text{N}_2\text{O}_5], \quad \text{where} \quad k_{hyd} = \frac{1}{4} \times \bar{c}_{\text{N}_2\text{O}_5} \times \text{SA} \times \gamma(\text{N}_2\text{O}_5). \quad \text{(A2)}$$

Here α is the< INF > < I > i < /I > < /INF > branching ratio for $RONO_2$ production from the reaction of NO_3 with alkenes, $\bar{c}_{N_2O_5}$ represents the mean molecular speed of N_2O_5, $\gamma(N_2O_5)$ represents the heterogeneous uptake coefficient for N_2O_5, and SA represents the aerosol surface area per volume of air.

We use the rate constant for the reaction ofNO_3 + isoprene for $k_{\text{NO}_3+\text{alkene}}$. Values for $k_{\text{NO}_3+\text{alkene}}$ and for k_b (defined below) are from the IUPAC chemical kinetics database (Atkinson et al., 2004, 2006). Values for $k_{\text{NO}_2+\text{O}_3}$ and for k_f are from JPL Data Evaluation #18 (Burkholder et al., 2015). We assume an initial mixing ratio of NO_2 (1 ppb), and constant O_3 (40 ppb), pressure (1013 hPa), and $\gamma(N_2O_5)$ (0.04). Additionally, we assume NO_3 and N_2O_5 in steady state:

$$[\text{NO}_3]_{SS} = \frac{k_{\text{NO}_2+\text{O}_3}[\text{NO}_2][\text{O}_3]}{k_{\text{NO}_3+\text{alkene}}[\text{alkene}]} \quad \text{(A3)}$$

$$[N_2O_5]_{SS} = \frac{k_f[NO_3][NO_2]}{k_b + k_{hyd}}, \quad \text{(A4)}$$

where k_f represents the formation of N_2O_5 from NO_2 and NO_3 and k_b represents the decomposition of N_2O_5 into NO_2 and NO_3.

Acknowledgments
This work was supported by NASA grant 80NSSC18K0624 and an NSF Graduate Research Fellowship to H.S.K. (DGE1106400). This material is based upon work supported by the National Center for Atmospheric Research, which is a major facility sponsored by the National Science Foundation under Cooperative Agreement No. 1852977. We thank the science teams of SEAC^{4}RS, FRAPPÉ, and KORUS-AQ. Data from SEAC^{4}RS are available at https://www-air.larc.nasa.gov/cgi-bin/ArcView/seac4rs. Data from FRAPPÉ are available at https://data.eol.ucar.edu/master_lists/generated/frappe/. Data from KORUS-AQ are available at https://www-air.larc.nasa.gov/cgi-bin/ArcView/korusaq?DC8=1.

References

Apel, E. C., Hornbrook, R. S., Hills, A. J., Blake, N. J., Barth, M. C., Weinheimer, A. J., et al. (2015). Upper tropospheric ozone production from lightning NO_x-impacted convection: Smoke ingestion case study from the DC3 campaign. *Journal of Geophysical Research: Atmosphere*, *120*, 2505–2523. https://doi.org/10.1002/2014JD022121

Atkinson, R., Baulch, D. L., Cox, R. A., Crowley, J. N., Hampson, R. F., Hynes, R. G., et al. (2004). Evaluated kinetic and photochemical data for atmospheric chemistry: Volume I - gas phase reactions of O_x, HO_x, NO_x and SO_x species. *Atmospheric Chemistry and Physics*, *4*(6), 1461–1738. https://doi.org/10.5194/acp-4-1461-2004

Atkinson, R., Baulch, D. L., Cox, R. A., Crowley, J. N., Hampson, R. F., Hynes, R. G., et al. IUPAC Subcommittee (2006). Evaluated kinetic and photochemical data for atmospheric chemistry: Volume II - gas phase reactions of organic species. *Atmospheric Chemistry and Physics*, *6*(11), 3625–4055. https://doi.org/10.5194/acp-6-3625-2006

Ayres, B. R., Allen, H. M., Draper, D. C., Brown, S. S., Wild, R. J., Jimenez, J. L., et al. (2015). Organic nitrate aerosol formation via NO_3+ biogenic volatile organic compounds in the southeastern United States. *Atmospheric Chemistry and Physics*, *15*(23), 13,377–13,392. https://doi.org/10.5194/acp-15-13377-2015

Brown, S. S., An, H., Lee, M., Park, J. H., Lee, S. D., Fibiger, D. L., et al. (2017). Cavity enhanced spectroscopy for measurement of nitrogen oxides in the Anthropocene: Results from the Seoul tower during MAPS 2015. *Faraday Discuss*, *200*, 529–557. https://doi.org/10.1039/c7fd00001d

Brown, S. S., Dubé, W. P., Peischl, J., Ryerson, T. B., Atlas, E., Warneke, C., et al. (2011). Budgets for nocturnal VOC oxidation by nitrate radicals aloft during the 2006 Texas Air Quality Study. *Journal of Geophysical Research*, *116*, D24305. https://doi.org/10.1029/2011JD016544

Burkholder, J. B., Sander, S. P., Abbatt, J. P. D., Barker, J. R., Huie, R. E., Kolb, C. E., et al. (2015). Chemical Kinetics and Photochemical Data for Use in Atmospheric Studies, Evaluation No. 18 (Tech. Rep.) Pasadena: Jet Propulsion Laboratory. https://jpldataeval.jpl.nasa.gov

Colbeck, I., & Harrison, R. M. (1985). Dry deposition of ozone: Some measurements of deposition velocity and of vertical profiles to 100 metres. *Atmospheres Environment*, *19*(11), 1807–1818. https://doi.org/10.1016/0004-6981(85)90007-1

Colman, J. J., Swanson, A. L., Meinardi, S., Sive, B. C., Blake, D. R., & Rowland, F. S. (2001). Description of the analysis of a wide range of volatile organic compounds in whole air samples collected during PEM-Tropics A and B. *Analytical Chemistry*, *73*(15), 3723–3731. https://doi.org/10.1021/ac010027g

Day, D. A., Dillon, M. B., Wooldridge, P. J., Thornton, J. A., Rosen, R. S., Wood, E. C., & Cohen, R. C. (2003). On alkyl nitrates, O_3, and the missing NO_y. *Journal of Geophysical Research*, *108*(D16), JD003685. https://doi.org/10.1029/2003JD003685

Day, D. A., Wooldridge, P. J., Dillon, M. B., Thornton, J. A., & Cohen, R. C. (2002). A thermal dissociation laser-induced fluorescence instrument for in situ detection of NO_2 , peroxy nitrates, alkyl nitrates, and HNO_3. *Journal of Geophysical Research*, *107*(D6), 4046. https://doi.org/10.1029/2001JD000779

Edwards, P. M., Aikin, K. C., Dubé, W. P., Fry, J. L., Gilman, J. B., De Gouw, J., et al. (2017). Transition from high- to low-NO_x control of night-time oxidation in the southeastern US. *Nature Geoscience*, *10*(7), 490–495. https://doi.org/10.1038/ngeo2976

Fisher, J. A., Jacob, D. J., Travis, K. R., Kim, P. S., Marais, E. A., Chan, C., et al. (2016). Organic nitrate chemistry and its implications for nitrogen budgets in an isoprene- and monoterpene-rich atmosphere : Constraints from aircraft (SEAC^{4}RS) and ground-based (SOAS) observations in the Southeast US. *Atmospheric Chemistry and Physics*, *16*, 5969–5991. https://doi.org/10.5194/acp-16-5969-2016

Flocke, F., Pfister, G., Crawford, J. H., Pickering, K. E., Pierce, G., Bon, D., & Reddy, P. (2020). Air quality in the northern colorado front range metro area: The front range air pollution and photochemistry Éxperiment (FRAPPÉ). *Journal of Geophysical Research: Atmospheres*, *125*, e2019JD031197. https://doi.org/10.1029/2019JD031197

Fry, J. L., Draper, D. C., Zarzana, K. J., Campuzano-Jost, P., Day, D. A., Jimenez, J. L., et al. (2013). Observations of gas- and aerosol-phase organic nitrates at BEACHON-RoMBAS 2011. *Atmospheric Chemistry and Physics*, *13*(17), 8585–8605. https://doi.org/10.5194/acp-13-8585-2013

Horowitz, L. W., Fiore, A. M., Milly, G. P., Cohen, R. C., Perring, A., Wooldridge, P. J., et al. (2007). Observational constraints on the chemistry of isoprene nitrates over the eastern United States. *Journal of Geophysical Research*, *112*, D12S08. https://doi.org/10.1029/2006JD007747

Huang, W., Saathoff, H., Shen, X., Ramisetty, R., Leisner, T., & Mohr, C. (2019). Chemical characterization of highly functionalized organonitrates contributing to night-time organic aerosol mass loadings and particle growth. *Environment Science Technology*, *53*(3), 1165–1174. https://doi.org/10.1021/acs.est.8b05826

Kenagy, H. S., Sparks, T. L., Ebben, C. J., Wooldrige, P. J., Lopez-Hilfiker, F. D., Lee, B. H., et al. (2018). NO_x lifetime and NO_y partitioning during WINTER. *Journal of Geophysical Research: Atmospheres*, *123*, 9813–9827. https://doi.org/10.1029/2018JD028736

Kiendler-Scharr, A., Mensah, A. A., Friese, E., Topping, D., Nemitz, E., Prevot, A. S. H., et al. (2016). Ubiquity of organic nitrates from nighttime chemistry in the European submicron aerosol. *Geophysical Research Letters*, *43*, 7735–7744. https://doi.org/10.1002/2016GL069239

Lee, Alex K. Y., Adam, M. G., Liggio, J., Li, S.-M., Li, K., Willis, M. D., et al. (2019). A large contribution of anthropogenic organo-nitrates to secondary organic aerosol in the Alberta oil sands. *Atmospheric Chemistry and Physics*, *19*, 12,209–12,219. https://doi.org/10.5194/acp-19-12209-2019

Lee, B. H., Mohr, C., Lopez-Hilfiker, F. D., Lutz, A., Hallquist, M., Lee, L., et al. (2016). Highly functionalized organic nitrates in the southeast United States: Contribution to secondary organic aerosol and reactive nitrogen budgets. *Proceedings of the National Academy of Science*, *113*(6), 1516–1521. https://doi.org/10.1073/pnas.1508108113

Lenschow, D. H., Pearson, R., & Stankov, B. B. (1981). Estimating the ozone budget in the boundary layer by use of aircraft measurements of ozone eddy flux and mean concentration. *Journal of Geophysical Research*, *86*(8 C), 7291–7297. https://doi.org/10.1029/jc086ic08p07291

Liebmann, J., Sobanski, N., Schuladen, J., Karu, E., Hellén, H., Hakola, H., et al. (2019). Alkyl nitrates in the boreal forest: Formation via the NO_3, OH and O_3 induced oxidation of BVOCs and ambient lifetimes. *Atmospheric Chemistry and Physics*, *3*, 1–23. https://doi.org/10.5194/acp-2019-463

Nault, B. A., Campuzano-jost, P., Day, D. A., Schroder, J. C., Anderson, B., Beyersdorf, A. J., et al. (2018). Secondary organic aerosol production from local emissions dominates the organic aerosol budget over Seoul, South Korea, during KORUS-AQ. *Atmospheric Chemistry and Physics*, *18*, 17,769–17,800. https://doi.org/10.5194/acp-18-17769-2018

Perring, A. E., Pusede, S. E., & Cohen, R. C. (2013). An observational perspective on the atmospheric impacts of alkyl and multifunctional nitrates on ozone and secondary organic aerosol. *Chemical Reviews*, *113*(8), 5848–5870. https://doi.org/10.1021/cr300520x

Pye, H. O. T., Luecken, D. J., Xu, L., Boyd, C. M., Ng, N. L., Baker, K. R., et al. (2015). Modeling the current and future roles of particulate organic nitrates in the Southeastern United States. *Environment Science Technology*, *49*(24), 14,195–14,203. https://doi.org/10.1021/acs.est.5b03738

Ridley, B. A., Walega, J. G., Dye, J. E., & Grahek, F. E. (1994). Distributions of NO, NO_x, NO_y, and O_3 to 12 km altitude during the summer monsoon season over New Mexico. *Journal of Geophysical Research*, *99*(D12), 25,519–25,534. https://doi.org/10.1029/94JD02210

Rollins, A. W., Browne, E. C., Min, K.-E., Pusede, S. E., Wooldridge, P. J., Gentner, D. R., et al. (2012). Evidence for NO_x control over nighttime SOA formation. *Science (80-.)*, *337*(6099), 1210–1212. https://doi.org/10.1126/science.1221520

Romer Present, P. S., Zare, A., & Cohen, R. C. (2020). The changing role of organic nitrates in the removal and transport of NO_x. *Atmospheric Chemistry and Physics*, *20*, 267–279. https://doi.org/10.5194/acp-20-267-2020

Ryerson, T. B., Huey, L. G., Knapp, K., Neuman, J. A., Parrish, D. D., Sueper, D. T., & Fehsenfeld, F. C. (1999). Design and initial characterization of an inlet for gas-phase NO_y measurements from aircraft. *Journal of Geophysical Research*, *104*(D5), 5483–5492.

Ryerson, T. B., Williams, E. J., & Fehsenfeld, F. C. (2000). An efficient photolysis system for fast-response NO_2 measurements. *Journal of Geophysical Research*, *105*(D21), 26,447–26,461. https://doi.org/10.1029/2000JD900389

Simpson, I. J., Akagi, S. K., Barletta, B., Blake, N. J., Choi, Y., Diskin, G. S., et al. (2011). Boreal forest fire emissions in fresh Canadian smoke plumes: $C_1 - C_{10}$ volatile organic compounds (VOCs), CO_2, CO, NO_2, NO, HCN, and CH_3CH. *Atmospheric Chemistry and Physics*, *11*, 6445–6463. https://doi.org/10.5194/acp-11-6445-2011

Sobanski, N., Thieser, J., Schuladen, J., Sauvage, C., Song, W., Williams, J., et al. (2017). Day- and night-time formation of organic nitrates at a forested mountain-site in South West Germany. *Atmospheric Chemistry and Physics*, *17*, 4115–4130. https://doi.org/10.5194/acp-17-4115-2017

Starn, T. K., Shepson, P. B., Bertman, S. B., Riemer, D. D., Zika, R. G., & Olszyna, K. (1998). Nighttime isoprene chemistry at an urban-impacted forest site. *Journal of Geophysical Research*, *103*(D17), 22,437–22,447. https://doi.org/10.1029/98JD01201

Toon, O. B., Maring, H., Dibb, J. E., Ferrare, R., Jacob, D. J., Jenson, E. J., et al. (2016). Planning, implementation, and scientific goals of the Studies of Emissions and Atmospheric Composition, Clouds and Climate Coupling by Regional Surveys ($SEAC^4RS$) field mission. *Journal of Geophysical Research: Atmospheres*, *121*, 4967–5009. https://doi.org/10.1002/2015JD024297

von Kuhlmann, R., Lawrence, M. G., Pöschl, U., & Crutzen, P. J. (2004). Sensitivities in global scale modeling of isoprene. *Atmospheric Chemistry and Physics*, *4*, 1–17. https://doi.org/10.5194/acp-4-1-2004

Weinheimer, A. J., Walega, J. G., Ridley, B. A., Gary, B. L., Blake, D. R., Blake, N. J., et al. (1994). Meridional distributions of NO_x, NO_y, and other species in the lower stratosphere and upper troposphere during AASE II. *Geophysical Research Letters*, *21*(23), 2583–2586. https://doi.org/10.1029/94GL01897

Wooldridge, P. J., Perring, A. E., Bertram, T. H., Flocke, F. M., Roberts, J. M., Singh, H. B., et al. (2010). Total peroxy nitrates (ΣPNs) in the atmosphere: The thermal dissociation-laser induced fluorescence (TD-LIF) technique and comparisons to speciated PAN measurements. *Atmosphere Measurement Technical*, *3*(3), 593–607. https://doi.org/10.5194/amt-3-593-2010

Xiong, F., McAvey, K. M., Pratt, K. A., Groff, C. J., Hostetler, M. A., Lipton, M. A., et al. (2015). Observation of isoprene hydroxynitrates in the Southeastern United States and implications for the fate of NO_x. *Atmospheric Chemistry and Physics*, *15*, 11,257–11,272. https://doi.org/10.5194/acp-15-11257-2015

Xu, L., Guo, H., Boyd, C. M., Klein, M., Bougiatioti, A., Cerully, K. M., et al. (2015). Effects of anthropogenic emissions on aerosol formation from isoprene and monoterpenes in the southeastern United States. *Proceedings of the National Academy of Science U. S. A.*, *112*(1), 37–42. https://doi.org/10.1073/pnas.1417609112

Xu, L., Suresh, S., Guo, H., Weber, R. J., & Ng, N. L. (2015). Aerosol characterization over the southeastern United States using high-resolution aerosol mass spectrometry: Spatial and seasonal variation of aerosol composition and sources with a focus on organic nitrates. *Atmospheric Chemistry and Physics*, *15*(13), 7307–7336. https://doi.org/10.5194/acp-15-7307-2015